Biomaterials 33 (2012) 8907–8916

Contents lists available at SciVerse ScienceDirect

Biomaterials

journal homepage: www.elsevier.com/locate/biomaterials

Arginine-rich self-assembling peptides as potent antibacterial gels

Ana Salomé Veiga [a,b], Chomdao Sinthuvanich [a,c], Diana Gaspar [b], Henri G. Franquelim [b], Miguel A.R.B. Castanho [b], Joel P. Schneider [a,*]

[a] Chemical Biology Lab, National Cancer Institute, Frederick, MD 21702, USA
[b] Instituto de Medicina Molecular, Faculdade de Medicina da Universidade de Lisboa, Av. Prof. Egas Moniz, 1649-028 Lisbon, Portugal
[c] Chemistry and Biochemistry Department, University of Delaware, Newark, DE 19716, USA

ARTICLE INFO

Article history:
Received 20 June 2012
Accepted 21 August 2012
Available online 17 September 2012

Keywords:
Peptide
Self-assembly
Hydrogel
Antibacterial
Syringe delivery

ABSTRACT

Hydrogel materials that display inherent activity against bacteria can be used to directly treat accessible wounds to prevent or kill existing infection. Hydrogels composed of self-assembling β-hairpin peptides, having a high content of arginine, were found to be extremely effective at killing both gram-positive and gram-negative bacteria, including multi-drug resistant *Pseudomonas aeruginosa*. No added antibacterial agents are necessary to realize activity. Using self-assembling peptides for material construction allows facile structure–activity relationships to be determined since changes in peptide sequence at the monomer level are directly transposed to the bulk material's antibacterial properties. SAR studies show that arginine content largely influences the hydrogel's antibacterial activity, and influences their bulk rheological properties. These studies culminated in an optimized gel, composed of the peptide PEP6R (VKVRVRVRV^{D}PPTRVRVRVKV). PEP6R gels prepared at 1.5 wt % or higher concentration, demonstrate high potency against bacteria, but are cytocompatible toward human erythrocytes as well as mammalian mesenchymal stem cells. Rheological studies indicate that the gel is moderately stiff and displays shear-thin recovery behavior, allowing its delivery via simple syringe.

Published by Elsevier Ltd.

1. Introduction

Bacterial infections are a common problem associated with dermal wounds [1,2]. These infections can prolong or impair wound healing, contributing to tissue morbidity and in extreme cases, result in sepsis. *Staphylococcus aureus* (*S. aureus*), *Escherichia coli* (*E. coli*) and *Pseudomonas aeruginosa* (*P. aeruginosa*) belong to a suite of bacteria commonly found in nosocomial infections [3,4]. *P. aeruginosa* is an especially bad actor, being the fourth most common nosocomial pathogen accounting for 10% of all hospital infections. *P. aeruginosa* infection remains a serious problem for patients hospitalized for cancer, AIDS, burns and cystic fibrosis [5–8].

Antibacterial hydrogels can be used to directly treat accessible wounds to prevent or kill existing infection. Hydrogels can be used to deliver small molecule antibiotics or the material, itself, can be designed to be the antibacterial agent, circumventing the need to encapsulate therapeutic [9–11]. For many material types, including gels, their surfaces can be endowed with antibacterial properties. This is typically accomplished by covalently immobilizing known antibiotics or fixing silver nanoparticles or quaternary ammonium groups to their surfaces [12–16]. Materials that inherently display polycationic surfaces are also known to be active against a broad spectrum of both Gram-positive and Gram-negative bacteria via a direct-contact mechanism involving bacterial membrane disruption [10].

We have shown that antibacterial hydrogels can be prepared from lysine-rich, self-assembling β-hairpin peptides. These peptides assemble into a polycationic fibrillar network capable of killing bacteria via a mechanism involving membrane disruption. When bacteria come in contact with the fibril surface, their membranes become comprised and this leads to cell death by lysis. An excellent feature of these materials is that the surface chemistry of their fibrillar networks can be varied by simply modulating the amino acid composition of the peptide monomer used for self-assembly [17,18]. This allows one to modify the structure of these gels at the nanometer length scale in efforts to create new materials with enhanced activity.

An excellent source of inspiration for the design of new, more effective materials is Nature. Antimicrobial peptides (AMPs) are a ubiquitous class of host defense molecules used across species. AMPs are small, water-soluble peptides that fold into amphiphilic conformations, typically helices and β-sheets, which display opposing hydrophobic and polycationic surfaces. The cationic face of an AMP is responsible for engaging the negatively charged, phospho-rich surface of the bacteria's membrane via hydrogen bonding and electrostatic interactions. Once bound to the outer-

* Corresponding author.
E-mail addresses: joel.schneider@nih.gov, schneiderjp@mail.nih.gov (J.P. Schneider).

0142-9612/$ – see front matter Published by Elsevier Ltd.
http://dx.doi.org/10.1016/j.biomaterials.2012.08.046

leaflet of the membrane, the hydrophobic face of the peptide facilitates peptide insertion into the lipid portion of the membrane, and through a myriad of possible mechanisms, ultimately disrupts the membrane, causing cell death. The polycationic surface of many AMPs contain a high content of arginine residues whose side chain guanidinium groups can establish strong bidentate hydrogen bonds and salt bridges with the phospho-rich membrane surface of bacteria. Thus, high arginine content often equates to strong lytic behavior for AMPs [19–23].

Herein, we describe the design and utilization of injectable gels prepared from arginine (Arg)-rich, self-assembling peptides to determine if the arginine-based activity enjoyed by so many AMPs can be taken advantage of and engineered into a self-assembled material. The importance of Arg and its guanidinium side chain to the antibacterial action of this class of gels was investigated by performing an SAR study where pairs of Arg residues within the peptide were replaced with the simple alkyl amine side chain of lysine (Lys).

2. Materials and methods

2.1. Materials

PL-rink amide resin was purchased from Varian and Fmoc-protected amino acids from NovaBiochem. 1H-Benzotriazolium 1-[bis(dimethylamino)methylene]-5-chloro-hexafluorophosphate (1-),3-oxide (HCTU) was purchased from Peptides International. Trifluoroacetic acid (TFA) was purchased from Acros. Thioanisole, anisole, acetonitrile, Bis-tris propane (BTP), 4-(2-Hydroxyethyl)piperazine-1-ethanesulfonic acid (HEPES), and calcium chloride dihydrate ($CaCl_2$) were purchased from Sigma–Aldrich. Ethanedithiol was from Fluka. Diethyl ether and sodium chloride (NaCl) were purchased from Fisher Scientific.

2.2. Peptide synthesis

Peptides were prepared on PL-Rink amide resin via automated Fmoc-based peptide synthesis on an ABI 433A peptide synthesizer with HCTU activation. Resin-bound peptide was cleaved and side chain-deprotected using a TFA:thioanisole:ethanedithiol:anisole (90:5:3:2) cocktail for 2 h under low Ar atmosphere. Filtration followed by cold ether precipitation yielded crude peptides. Crude peptides were purified by RP-HPLC using a preparative Vydac C18 peptide column. Purification of all peptides was performed at 40 °C employing an isocratic gradient. PEP8R gradient: 0% B for 2 min, then a linear gradient from 0 to 10% B over 6 min, then 10%–100% B over 186 min. Peptide elutes at 30% B. PEP6R gradient: 0% B for 2 min, then a linear gradient from 0 to 9% B over 5 min, then 9%–100% B over 187 min. Peptide elutes at 29% B. PEP4R gradient: 0% B for 2 min, then a linear gradient from 0 to 14% B over 8 min, then 14%–100% B over 180 min. Peptide elutes at 29% B. PEP2R gradient: 0% B for 2 min, then a linear gradient from 0 to 14% B over 8 min, then 14%–100% B over 180 min. Peptide elutes at 28% B. D-PEP6R gradient: 0% B for 2 min, then a linear gradient from 0 to 9% B over 6 min, then 9%–100% B over 188 min. Peptide elutes at 29% B. PEP6RE gradient: 0% B for 2 min, then a linear gradient from 0 to 13% B over 6 min, then 13%–100% B over 180 min. Peptide elutes at 33% B. Elutants for RP-HPLC consisted of Standard A (0.1% TFA in water) and Standard B (90% acetonitrile, 9.9% water, 0.1% TFA). Analytical HPLC chromatograms and ESI (+) mass spectra for the pure peptides are shown in the Supplementary Material.

2.3. CD spectroscopy

Circular dichroism (CD) spectra were collected on an AVIV model 420 circular dichroism spectrometer. For all peptides, spectra were collected in both water and BTP buffer at 1 wt%. Wavelength scans were performed from 200 to 260 nm at 37 °C using a 0.1 mm pathlength quartz cell. For the experiments in water, 150 μL of a 1 wt % peptide stock solution in chilled water was placed in the CD cell. For measurements in buffer, 100 μL of a 2 wt% peptide stock solution in chilled H_2O was first prepared, followed by the addition of 100 μL chilled BTP buffer (100 mM, 300 mM NaCl, pH 7.4), resulting in a 1 wt% peptide solution. 150 μL of this solution was quickly transferred to the cell and allowed to gel. The mean ellipticity, $[\theta]$, was calculated from the equation $[\theta] = (\theta_{obs}/10lc)/r$, where θ_{obs} is the measured ellipticity (mdeg), l is the length of the cell (cm), c is the molar concentration, and r is the number of residues.

2.4. Oscillatory rheology

Oscillatory rheology experiments were performed on an ARG2 rheometer (TA Instruments) using a 25 mm stainless steel parallel plate geometry. For hydrogel preparation, 175 μL of a 2 wt% peptide stock solution was prepared in chilled H_2O in a cylindrical glass vial. Then, 175 μL of BTP buffer (100 mM, 300 mM NaCl, pH 7.4) was added. 300 μL of the resultant 1 wt% peptide solution was quickly transferred to the rheometer plate, which was pre-equilibrated at 5 °C. The parallel plate tool was then lowered to a gap height of 0.5 mm and the temperature was ramped linearly to 37 °C to initiate folding and self-assembly (100 s). For the gelation experiments a dynamic time sweep was performed at 37 °C (6 rad/s, 0.2% strain) for 1 h to monitor the storage modulus (G′) and loss modulus (G″) over time for each peptide.

In the shear-thin and recovery experiments, PEP6R gels were prepared as described for oscillatory rheology experiments. Here, a dynamic time sweep was performed at 6 rad/s, 0.2% strain first. Then, 1000% strain was applied for 30 s to disrupt the hydrogel network at a frequency of 6 rad/s. This was followed by another 1 h dynamic time sweep (6 rad/s, 0.2% strain) to measure the hydrogel moduli recovery after shear.

2.5. Antibacterial assays

Hydrogels in the antibacterial assays were prepared in separate wells of 96-well tissue cultured-treated polystyrene plate (TCTP, Costar 3595). For a given peptide, four different wells were prepared at four different weight percentages: 0.5, 1, 1.5, and 2 wt%. To each well, 35 μL of a peptide stock solution in sterile filtered H_2O (1, 2, 3, and 4 wt%) was introduced, followed by the addition of 35 μL of BTP buffer (100 mM, 300 mM NaCl, pH 7.4) to initiate gelation. The resulting hydrogels (0.5, 1, 1.5, and 2 wt%) were incubated at 37 °C for 3 h in a humidified incubator. Then an additional 200 uL of BTP buffer (50 mM, 150 mM NaCl, pH 7.4) was added to the top of the gels, and the gels were equilibrated overnight at 37 °C. Prior to the start of the assay, the buffer was removed from the top of the hydrogels.

The bacterial strains used for the studies included: *E. coli* (ATCC 25922), *S. aureus* (ATCC 25923) and *P. aeruginosa* (ATCC 27853) purchased from American Type Culture Collection. Bacteria were grown on Trypticase™ Soy Agar plates with 5% sheep blood (BBL 221239) overnight (18–20 h) at 37 °C prior to the hydrogel assays. For each bacterial strain, solutions of 10^4 CFU/mL were prepared in Tryptic Soy Broth (TSB, BD 211824). A 100 μL aliquot of the 10^4 CFU/mL bacterial stock solution was introduced to the surface of each hydrogel, resulting in final bacterial concentration of 10^5 CFU/dm^2 on the gel surface. Bacteria were incubated for 24 h on the hydrogel surfaces, as well as a TCTP surface (as a control) at 37 °C. The following day, 100 μL of bacteria-free TSB was added to the surfaces to gently wash and remove the assay solution for measurement. Bacterial growth was monitored by measuring the $OD_{625\ nm}$ of the solution above the gel. Corrected $OD_{625\ nm}$ was calculated to account for dilution and to normalize the scattering for each individual bacterial strain [17]. Each assay was performed in triplicate for all bacterial strains. Antibacterial activity is represented as percent non-viable bacteria, where % non-viable bacteria $= [1 - (OD_{625}\ surface/OD_{625}\ control)] \times 100$.

2.6. Hemolytic assays

Peptides hydrogels at different weight percentages (0.5, 1, 1.5, and 2 wt%) were prepared in a 96-well TCTP plate as described above for the antibacterial assays. The hemolytic activity of the hydrogels was determined using human red blood cells (hRBCs). Blood was obtained from the Frederick Research Donor Program. The hRBCs were washed three times with BTP buffer (50 mM, 150 mM NaCl, pH 7.4) by centrifugation for 10 min at 3460 rpm and 4 °C. Then, 30 μL of hRBCs were suspended in 12 mL of BTP buffer (50 mM, 150 mM NaCl, pH 7.4) resulting in a 0.25% (v/v) suspension. 80 μL of the hRBCs stock solution was introduced to individual TCTP control and hydrogels surfaces, followed by the addition of 170 μL of BTP buffer to the top of each well for a final volume of 250 μL corresponding to a 0.08% (v/v) hRBCs. Samples were then incubated at 37 °C with agitation for 1 h. After which time, the solution on the top of the surfaces was removed and centrifuged at 14,000 rpm for 10 min at 4 °C. Hemolytic activity was assessed by determining the amount of hemoglobin that was released as a result of cell membrane rupture. The release of hemoglobin was measured via the absorbance of the supernatant at 415 nm. Controls for 0 and 100% hemolysis were defined by adding BTP buffer and a 1% Triton X-100 solution to hRBCs on the control surface, respectively. Each assay was performed in triplicate.

2.7. Bacterial live-dead assay

Hydrogels in the bacterial viability assay were prepared in separate wells of an 8-well borosilicate glass confocal plate (Nunc 155409). To each well 75 μL of a 4 wt% PEP6R stock solution was introduced followed by the addition of 75 μL of BTP buffer (100 mM, 300 mM NaCl, pH 7.4) to initiate gelation. The resulting 2 wt% hydrogels were incubated at 37 °C for 3 h in a humidified incubator. Then an additional 400 uL of BTP buffer (50 mM, 150 mM NaCl, pH 7.4) was added to the top of the gels, and the gels were equilibrated overnight at 37 °C. Prior to the start of the assay, the buffer was removed from the top of the hydrogels.

A 200 μL aliquot of a *P. aeruginosa* 10^4 CFU/mL stock solution, prepared as described before, was introduced to the surface of each hydrogel, resulting in a final bacterial concentration of 10^5 CFU/dm^2 on the gel surface. Bacteria were also introduced on a borosilicate glass surface as a control. Following 24 h incubation at 37 °C, 200 μL of a Live-Dead BacLight (Molecular Probes, L7012) solution, prepared according to instructions, was added to each well resulting in a final concentration of

6 μM SYTO9 and 30 μM propidium iodide. Following incubation for 15 min at room temperature, bacteria were imaged using a 20× magnification on a Zeiss NLO510 laser scanning confocal microscope. Experiments were performed in triplicate.

2.8. Atomic force microscopy imaging

For the Atomic Force Microscopy (AFM) imaging of *E. coli* in the presence of PEP6R, 100 μL of 2 wt% gels were prepared as described before, on a Poly-L-Lysine slide inside an O-ring positioned in the center of the slide. An *E. coli* stock solution of 10^8 CFU/mL was prepared. Then, bacteria were centrifuged at 13,000 rpm for 8 min, and washed twice under the same conditions using sterile BTP buffer (50 mM, 150 mM NaCl, pH 7.4). The final bacterial suspension (at 10^7 CFU/mL) was prepared in BTP buffer. A 400 μL aliquot of the bacterial solution (10^7 CFU/mL) was added on the hydrogel's surface and incubated for 2 h at 37 °C. As a control, a 400 μL aliquot of the bacterial solution was incubated on the Poly-L-Lysine slide without gel. After incubation, bacteria were gently removed from the gel's surface. Gels were immediately rinsed 10 times with 200 μL of filtered water and left to dry. On average, five individual bacterial cells were imaged at high resolution.

The AFM images were acquired using a JPK Nano Wizard II (Berlin, Germany) mounted on a Zeiss Axiovert 200 inverted microscope (Göttingen, Germany). Measurements were carried out in intermittent contact mode using uncoated silicon ACL cantilevers from Applied NanoStructure (Santa Clara, CA, USA). ACL cantilevers had typical resonance frequencies between 145 and 230 kHz and an average spring constant of 45 N/m. Height and error images were recorded and images were line-fitted as required. Height and size information were acquired with the imaging software from JPK Instruments.

2.9. Antibacterial assays in the presence of Ca^{2+}

To study the antibacterial activity of PEP6R in the presence of Ca^{2+}, hydrogels were prepared in separate wells of 96-well TCTP plates, at 1 wt% as described before in the antibacterial assays section.

The bacterial strains used for the study, *E. coli* and *S. aureus*, were grown as described before. For each bacterial strain, solutions of 10^6 CFU/mL were prepared in BTP buffer (50 mM, 150 mM NaCl, pH 7.4). $CaCl_2$ from a stock solution was added in order to obtain bacterial solutions (final concentration of 10^4 CFU/mL) containing different concentrations of $CaCl_2$ (0.1, 1, 10 and 20 mM). A 100 μL aliquot of each solution was introduced to the surface of each hydrogel. Bacteria in the presence of Ca^{2+} were incubated for 2 h on the hydrogel surfaces, as well as a TCTP surface (as a control) at 37 °C. A 50 μL aliquot of the bacterial solution was removed from the surface of each hydrogel and diluted in BTP buffer. A 100 μL aliquot of this diluted solution was transferred to an agar plate. The CFU obtained were counted after 24 h incubation at 37 °C. Experiments were performed in triplicate. Antibacterial activity is represented as percent non-viable bacteria, where % non-viable bacteria = [1 − (Number of colonies $_{surface}$/Number of colonies $^{2+}_{control,\ 0\ mM\ Ca}$)] × 100.

2.10. Cytocompatibility assay

For mammalian cells assays, a 110 μL, 4 wt% PEP6R stock solution in chilled HEPES buffer (25 mM, pH 7.4) was prepared. To the stock, 110 μL chilled DMEM (Dulbeccos Modified Eagles Medium, supplemented with 25 mM HEPES, Gibco 12430) was added, resulting in a 2 wt% peptide solution. 200 μL of this solution was quickly transferred to one of the wells of an 8-well borosilicate glass confocal plate (Nunc 155409). PEP6R hydrogels were incubated for 3 h at 37 °C in 5% CO_2. Then, an additional 400 μL of DMEM (supplemented with 25 mM HEPES) was added on the top of the hydrogels and incubated overnight at 37 °C in 5% CO_2.

C3H10t1/2 murine mesenchymal stem cells (ATCC CCL-226) were cultured in growth media (DMEM, 10% heat-inactivated fetal bovine serum, 2 mM L-glutamine, 50 μg/mL gentamicin) at 37 °C in 5% CO_2. C3H10t1/2 were maintained on TCTP plates, then trypsinized, and counted using a hemacytometer. For the assay, a cell suspension was plated at a density of 20,000 cells/cm^2 on the control borosilicate plate and PEP6R hydrogels surfaces, and incubated for 24 h at 37 °C in 5% CO_2. The media above each surface was then removed and the surface washed with DMEM (supplemented with 25 mM HEPES). Cell viability was assessed by using a Live-Dead assay. Here, a stock solution containing both 1 μM calcein AM and 2 μM ethidium homodimer in DMEM supplemented with 25 mM HEPES was prepared according to the Live/Dead assay instructions (Molecular Probes, L3224). 200 μL of this solution was introduced onto the hydrogel and control surfaces and incubated at 37 °C for 5 min. For the negative control, a Triton X-100 solution was added to a final concentration of 0.1% before addition of the dye solution. Samples were imaged using a Zeiss NLO510 laser scanning confocal microscope equipped with Plan-Neofluar 10 ×/0.3 objective lens. Experiments were performed in triplicate.

3. Results and discussion

3.1. Peptide design

PEP8R was designed to self-assemble into a mechanically rigid antibacterial hydrogel and serve as the parent peptide from which structure-activity studies could be initiated. This peptide (VRVRVRVRV^DPPTRVRVRVRV-NH_2) contains twenty residues, eight of which are arginines. As will be shown, the peptide adopts an ensemble of random coil conformations when dissolved in water, but folds into an amphiphilic β-hairpin conformation that is highly amenable to self-assembly when folding is triggered by the addition of buffer containing NaCl. When dissolved in water, the arginine side chains are protonated and inter-residue charge repulsion keeps the peptide from folding. However, when buffer (pH 7) containing NaCl is added to the solution, the arginine-borne charge is screened and the peptide folds. In its folded state, PEP8R contains two β-strands of alternating valine (Val) and arginine (Arg) residues connected by a four residue type II′, β-turn sequence (-V^DPPT-). Each β-strand was designed to contain eight residues base on a report by Gellman et al. that showed that at least seven residues are necessary for optimal hairpin stability [24]. The alternating hydrophobic and hydrophilic residues of the strands impart amphiphilicity to the folded hairpin. The four residues occupying the β-turn were chosen based on their ability to adopt dihedrals consistent with conical type II′ turns found in naturally occurring proteins. The folded hairpin undergoes rapid self-assembly into a β-sheet rich fibrillar network leading to hydrogel formation, Fig. 1. Folding and self-assembly can be followed by monitoring the evolution of β-sheet secondary structure. Fig. 2A shows circular dichroism (CD) spectra of PEP8R in water and in the presence of buffer containing NaCl. In water the spectrum in consistent with unfolded peptide. However, in buffer the spectrum indicates that the peptide has folded and assembled into β-sheet structures.

PEP8R is designed to assemble into a fibrillar network where each fibril is composed of a bilayer of β-hairpins that

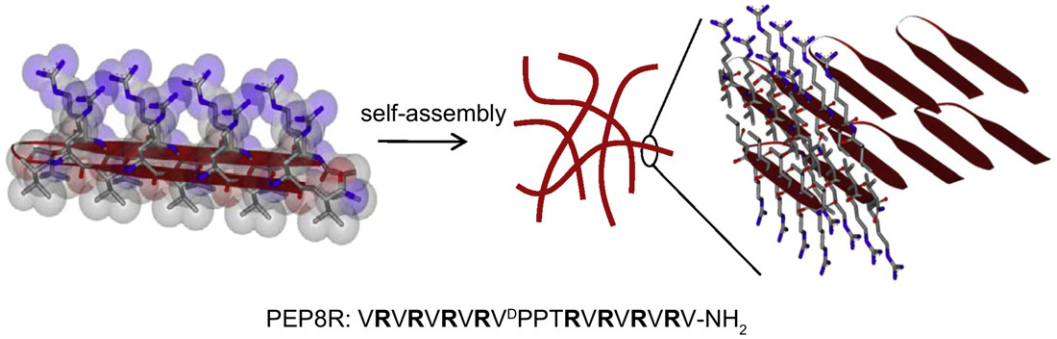

Fig. 1. Amphiphilicstructure of PEP8R hairpin designed to self-assemble into β-sheet rich fibrils that define the network of a syringe-deliverable hydrogel. Fibrils are comprised of a bilayer of hairpins that hydrogen-bond along the long-axis of a given fibril. The solvent-exposed fibril surfaces display a high concentration of arginine side chains. The PEP8R sequence is shown.

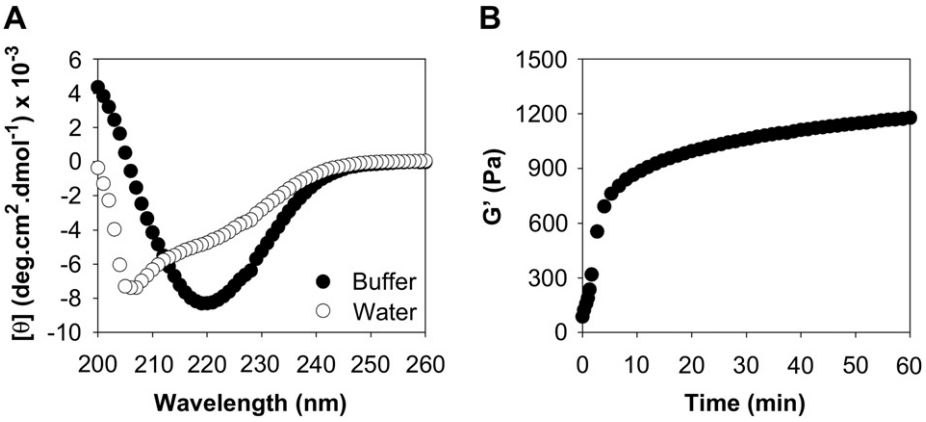

Fig. 2. (A) CD wavelength spectra of 1 wt% PEP8R in water and in the presence of BTP buffer at 37 °C. (B) Oscillatory rheological dynamic time sweep of 1 wt% PEP8R gel, monitoring the evolution of storage modulus (G′) as a function of time after gelation is initiated by the addition of buffer (50 mM BTP, 150 mM NaCl, pH 7.4) at 37 °C.

intermolecularly hydrogen bonds along the long-axis of the fibril, Fig. 1. Bilayer formation between hairpins is driven by the hydrophobic effect where the Val-rich faces of individual hairpins facially assemble to release ordered water and shield the hydrophobic face from bulk water. This mechanism of self-assembly is similar to that experimentally observed for other amphiphilic peptides studied in our lab [25,26] and leads to moderately rigid viscoelastic gels. Fig. 2B shows a dynamic time sweep experiment employing oscillatory rheology, were the storage modulus (G′, a measure of the material's mechanical rigidity) is measured as a function of time, on the addition of a saline buffer solution (pH 7.4) to a solution of unfolded peptide. The addition of buffer triggers peptide folding, self-assembly, leading to a gel characterized by a storage modulus of about 1200 Pa. The onset of gelation occurs rapidly over the first few minutes resulting in gel that stiffens over time. Important for this study, each fibril formed in the network displays a large concentration of solvent-exposed, positively charged Arg residues that can serve as potential warheads for bacterial engagement.

Given the known key role of arginine content in the activity of many AMPs [19–23], a gel prepared from PEP8R is expected to display potent antibacterial activity. In order to probe the importance of arginine and its guanidinium side chain to the antibacterial action of the PEP8R gel, we sequentially replaced pairs of Arg residues within each peptide of the fibril network with cationic Lys residues, Fig. 3A. To accomplish this, three addition self-assembling peptides were designed from the parent peptide, PEP8R, where the number of Arg residues varies from six to two. Their sequences are defined in Fig. 3B. Arg residues are progressively replaced by pairs of Lys residues, beginning from the peptide termini of PEP8R toward the turn region of the hairpin. Fig. 3C shows the measured storage moduli for 1 wt% preparations of each gel after 1 h incubation. Decreasing the number of arginine residues to 6 (PEP6R) results in an increase in mechanical rigidity. However, further reduction in arginine content results in a decrease of rigidity with PEP2R having a G′ of about 600 Pa.

3.2. Antibacterial activity of hydrogel surfaces

The antibacterial activity of each peptide hydrogel surface was first tested against cultures of *E. coli* and *S. aureus*, representative Gram-negative and Gram-positive bacteria, respectively. Both bacteria strains are common in hospital-acquired infections [3,4]. In these experiments, peptide gels were prepared in a manner that allowed the concentration of cationic side chain to be varied. For each peptide, gels of differing weight percent (0.5, 1, 1.5, and 2) were formulated. As the wt % increases, so does the concentration of cationic side chain displayed in the gel's network. Hydrogel surfaces were challenged with an inoculum of 10^5 CFU/dm^2 and viability measured after 24 h. Assessing activity in this manner is reminiscent of measuring the MIC for water soluble AMPs. As the concentration of peptide in the network increases, the antibacterial activity of the

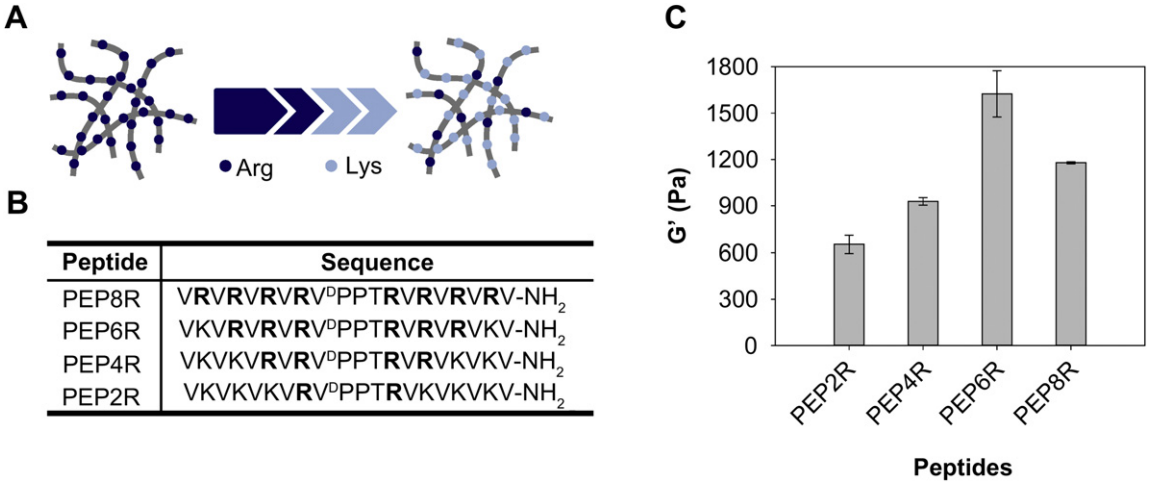

Peptide	Sequence
PEP8R	V**R**V**R**V**R**V^{D}PPT**R**V**R**V**R**V**R**V-NH$_2$
PEP6R	VKV**R**V**R**V**R**V^{D}PPT**R**V**R**V**R**VKV-NH$_2$
PEP4R	VKVKV**R**V**R**V^{D}PPT**R**V**R**VKVKV-NH$_2$
PEP2R	VKVKVKV**R**V^{D}PPT**R**VKVKVKV-NH$_2$

Fig. 3. (A) Structure–activity relationship for the fibril network is investigated by preparing a family of gels where arginine is gradually replaced with lysine. (B) Peptide sequences studied. (C) Average storage moduli of 1 wt% peptide gels after 1 h gelation (50 mM BTP, 150 mM NaCl, pH 7.4) at 37 °C.

gel should also increase. Hydrogels prepared from PEP8R were first examined. The PEP8R hydrogel surfaces are capable of inhibiting both *E. coli* and *S. aureus* proliferation, irrespective of the peptide weight percentage used (Fig. 4). The high content of Arg side chains on the surface of the fibrils was sufficient to afford a material with high antibacterial activity even for a gel prepared from as little as 0.5 wt% peptide. It was not possible to study gels of lower weight percent because 0.5 wt% is approaching the threshold of peptide concentration necessary to form the self-assembled gel.

Similar antibacterial assays were performed with the other Arg-containing peptide hydrogels. For gels prepared from PEP6R and PEP4R, where the Arg content was reduced to six and four Arg residues, respectively, the results obtained are similar. Fig. 4 shows that gels prepared from either peptide inhibit *E. coli* and *S. aureus* proliferation at all weight percentages. When the Arg content is reduced to only two Arg residues (PEP2R), the activity against *E. coli* (Fig. 4A) is diminished. At 0.5 wt% the hydrogel surface of PEP2R shows minimal action. However, as the wt% is increased, the gel surface gains activity in a wt%-dependent manner. For example, 2 wt% gels inhibit proliferation of about 50% of the introduced bacteria as compared to about 10% in the 0.5 wt% gel. This data shows that the Arg content influences the antibacterial activity of these gels against *E. coli*, and importantly, more than two Arg residues are needed to have gels that are effective at inhibiting *E. coli* proliferation.

As for Gram-positive bacteria, Fig. 4B shows that PEP2R gels are active against *S. aureus* and are able to inhibit its proliferation at all weight percentages used. This indicates that the hydrogel surfaces are more effective at inhibiting Gram-positive than Gram-negative bacteria proliferation, in accordance to results previously observed for other antimicrobial surfaces [27,28]. This preference is most likely due to differences in cell surface composition of the bacterial species, namely negatively charged lipid content [29–31]. Overall, the antibacterial assays show that PEP8R, PEP6R, and PEP4R are effective at inhibiting both Gram-negative and Gram-positive bacteria strains, and that a minimum of four Arg residues among a background of Lys residues are necessary for potent activity.

3.3. Hemolytic activity of hydrogels surfaces

Previous studies in our lab have shown that when bacteria come in contact with a polycationic surface their membranes become compromised [17]. Although the composition of mammalian membranes is distinct from bacteria, the potential for lytic activity still exists. To assess the biocompatibility of the gels, the hemolytic behavior of the Arg-containing materials toward hRBCs, model mammalian cells, was studied. A hRBC solution was introduced to the surface of the gels, and TCTP control surfaces. After 1 h incubation at 37 °C, cell lysis was monitored. Fig. 5A shows the results obtained for 2 wt% gels and controls. Only 2 wt% gels, as opposed to

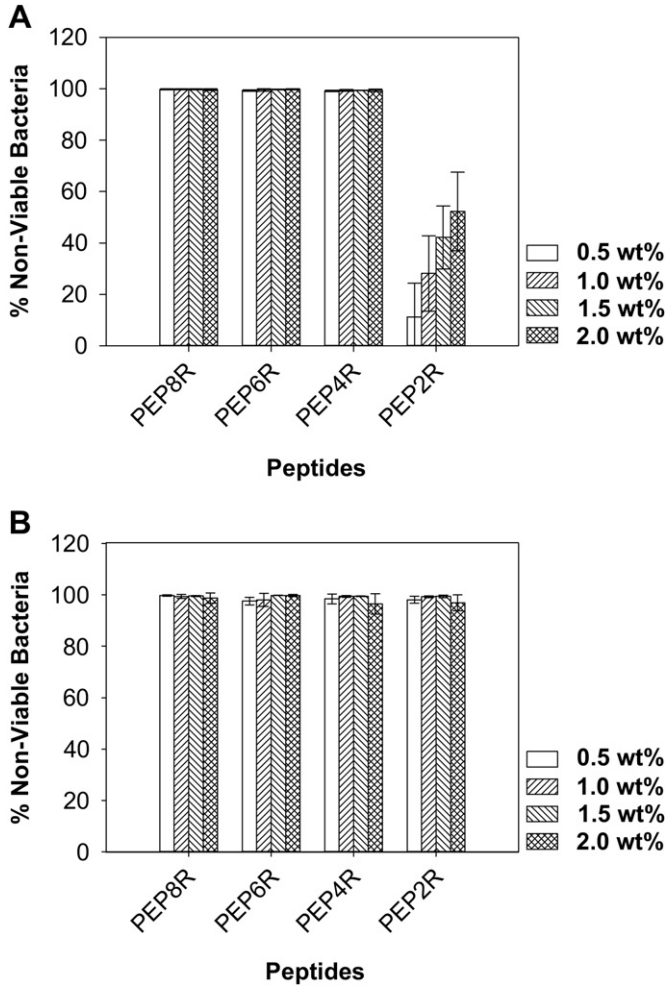

Fig. 4. Antibacterial activity of hydrogel surfaces against *E. coli* (A) and *S. aureus* (B) after 24 h incubation at 37 °C. Percent non-viable bacteria is reported for 0.5, 1, 1.5, and 2 wt% hydrogels ($n = 3$).

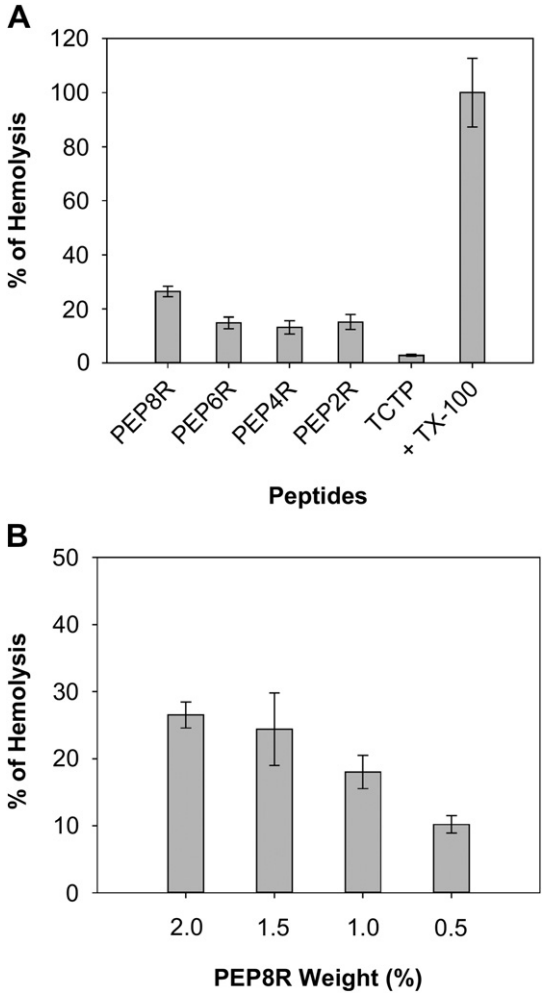

Fig. 5. (A) Hemolytic activity of 2 wt% peptide hydrogel surfaces. (B) Hemolytic activity of the PEP8R hydrogel as a function of wt%. Addition of 1% of Triton X-100 to hRBCs on TCTP represents 100% hemolysis. $n = 3$.

lower wt% gels, were initially examined since their hemolytic potential should be greatest. The PEP8R gel surface shows the highest hemolytic activity of about 25%. When the Arg content of the peptide used to prepare the gels is reduced, the hemolytic activity decreases considerably. PEP6R, PEP4R, and PEP2R gels display low hemolytic activity. To further demonstrate that the Arg content is largely responsible for the hemolytic activity of these gels, additional experiments were performed where PEP8R gels of varying wt% were examined. Fig. 5B shows that as the weight percent is decreased from 2 to 0.5, the hemolytic activity of the gel also decreases in a concentration dependent manner. This data strongly suggests that the Arg side chain is largely responsible for the hemolytic activity of the gel's surface. The antibacterial as well as the hemolytic data of all the peptide gels suggest that peptides containing between four and six Arg will have optimal utility, balancing antibacterial potency with low hemolytic activity.

3.4. Mechanistic investigations

The mechanism of action of these hydrogels against *E. coli*, *S. aureus* and the multi-drug resistant *P. aeruginosa* was investigated using PEP6R as a representative gel. *P. aeruginosa* was also included given its clinical importance. This gram-negative bacterium accounts for about ten percent of all nosocomial infections and is a serious problem for patients hospitalized with cancer, AIDS, burns and cystic fibrosis. PEP6R hydrogel surfaces of varying weight percents were challenged with 10^5 CFU/dm^2 of *P. aeruginosa* for 24 h at 37 °C. Fig. 6 shows that at 0.5 wt%, the PEP6R gel is only marginally active against *P. aeruginosa*. However, as the wt% is increased, the activity of the material's surface also increases with 1.5 and 2 wt% gels being extremely potent against this resistant strain. The concentration dependent nature of the data strongly suggests that the Arg content is largely responsible for the gel's activity.

The general mechanism by which PEP6R exerts its action was investigated by performing a live-dead assay using *P. aeruginosa*. The gel surface could be either cytostatic, simply inhibiting proliferation of existing cells, or cytotoxic, killing existing cells. Bacteria were introduced onto the surface of a 2 wt% hydrogel and incubated for 24 h. After which time, the assay was performed. Fig. 7 shows a z-stack confocal image, viewing cells perpendicular to the *z*-axis of the sample, along the interface between the gel surface and the tryptic soy broth. In this assay, dead cells fluoresce red and live cells fluoresce green. Bacterial cells at the material interface fluoresce red indicating that the gel surface is cytotoxic. The image in Fig. 7 provides additional insight into the gel's mechanism of action. The dye used to visualize dead cells, propidium iodide, is a membrane impermeant DNA intercalating agent. It can only stain cells whose membranes have been comprised. This suggests that as bacterial cells engage the hydrogel's surface, their membranes become comprised. For antibacterial agents known to work through membrane lytic mechanisms, membrane disruption events occur quickly [32]. Thus, an additional live-dead assay was performed in which the bacteria were incubated in the presence of the gel for only 2 h, as opposed to 24 h. The results were identical, further supporting a membrane lytic mechanism, See Supplementary Material.

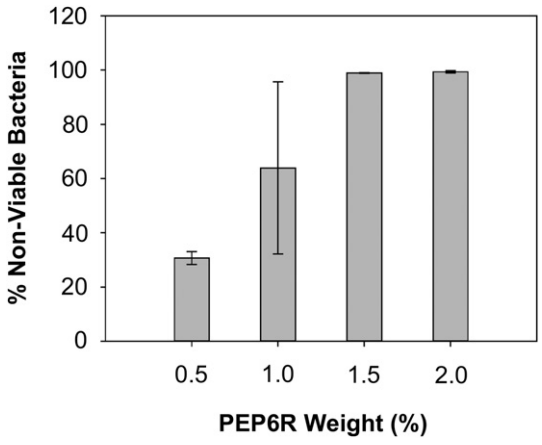

Fig. 6. Antibacterial activity of PEP6R hydrogel surface against *P. aeruginosa* after 24 h incubation at 37 °C. Percent non-viable bacteria is reported for 0.5, 1, 1.5, and 2 wt% hydrogels ($n = 3$).

Membrane lytic mechanisms are typically stereochemically non-specific. This is in contrast to antibacterial agents that bind to specific cell receptors to exert their activity. To provide additional evidence that the PEP6R gel acts through a stereochemically non-specific membrane disruption mechanism, the antibacterial activity of its enantiomeric gel was studied. D-PEP6R is the mirror image peptide of PEP6R and contains nearly all D-residues. If the mechanism of action for the L-hydrogels depends on a specific receptor-binding interaction, the D-PEP6R gel will be inactive. Fig. 8A and B shows the antibacterial activity of the D-PEP6R gel against *E. coli* and *S. aureus*, respectively. The results show that the antibacterial activity of the D-hydrogel is similar to that of the L-PEP6R gel (Fig. 4A and B) and suggests that the mechanism of action for these gels, in general, is similar for both gram-negative and -positive bacteria, namely a mechanism involving non-stereospecific membrane disruption.

The membrane disrupting activity of the PEP6R gel was further investigated by directly visualizing the morphology of *E. coli* that have come in contact with the gel's surface by AFM. Fig. 9A shows a representative image of an *E. coli* bacterium incubated for 2 h on the surface of a 2 wt % PEP6R gel. Although the cell retains its rod-like morphology, its membrane surface has collapsed and appears highly punctated. In contrast, Fig. 9B shows an *E. coli* bacterium incubated on a control poly-Lysine surface, its membrane fully intact.

The AFM data coupled with the fact that the D-hydrogel is active indicates a mechanism involving membrane disruption. Given the cationic nature of the hydrogel's surface, electrostatic interactions between the surface of the gel and the negatively charged bacterial membrane could prove to be important and are expected to form when the bacteria first engage the gel's surface. The importance of the PEP6R gel's positive charge content on its antibacterial activity was investigated by assessing the activity of an additional gel, which is less electropositive. PEP6RE is a derivative of PEP6R where an Arg residue at position 15 was replaced by a glutamic acid residue. The net formal charge of PEP6RE at neutral pH is +7 per monomer, whereas the charge of PEP6R is +9 per monomer. Thus, self-assembled networks of PEP6RE are significantly less electropositive as compared to networks formed by PEP6R.

PEP6RE hydrogel surfaces were challenged with a bacterial inoculum of 10^5 CFU/dm^2 and viability measured after 24 h. Fig. 10A and B shows the antibacterial activity of the PEP6RE gel as a function of wt % against *E. coli* and *S. aureus*, respectively. For *E. coli*, the activity of the PEP6RE hydrogel increases as the weight percent increases and importantly, the surface is not able to completely inhibit bacterial proliferation at any weight percent tested. This result is in direct contrast to the activity of the PEP6R gel, which quantitatively kills *E. coli* at all weight percents tested. These results are mirrored for *S. aureus*, where the activity of the PEP6RE gel increases with weight percent and only the highest weight percent gels being fully active. Again, this is in contrast to the gels prepared from the more electropositive PEP6R. These results suggest that surface electrostatics plays a role in the lytic potential of the hydrogel.

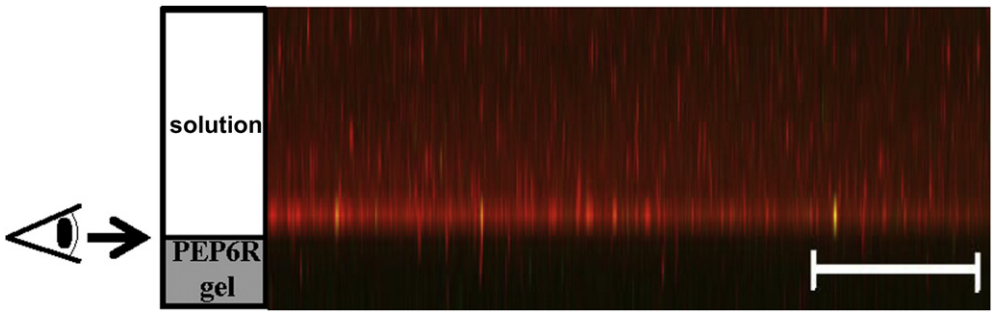

Fig. 7. LSCM Z-projection taken of 10^5 CFU/dm^2 *P. aeruginosa* incubated on a 2 wt% PEP6R hydrogel surface after 24 h incubation, viewed from the side of a gel along the interface between the gel surface and the tryptic soy broth. Green and red fluorescence denotes live and dead cells, respectively. (Scales bars: 100 μm; $n = 3$).

Divalent metal ions such as Ca^{2+} and Mg^{2+} are known to bind to, and stabilize macromolecular components of bacterial cell walls such as lipopolysaccharide and teichoic acid [33]. In fact, chelators, such as EDTA, are effective at killing bacteria, presumably by stripping the bacteria of these necessary components [33]. It is plausible that the highly electropositive fibrils comprising the gel network may be acting in a similar fashion. As bacteria come into contact with the gel's surface, their divalent metal ions might shed via electrostatic repulsion as the electropositive fibrils engage the cell wall. Thus, release of essential metal ions may be the first step in initiating cell death. This hypothesis was tested by performing Ca^{2+} ion-dependent antibacterial assays for the PEP6R gel. In this experiment, PEP6R hydrogel surfaces were challenged with an inoculum of 10^5 CFU/dm^2 in the presence of increasing concentrations of Ca^{2+}. If the gel surface is actively displacing divalent metal ions and this contributes to cell death, then the activity of the gel should be titrated with increasing concentrations of free calcium. The results for *E. coli* and *S. aureus* are show in Fig. 11A and B, respectively and show that the gel's antibacterial activity is progressively attenuated with increasing concentrations of Ca^{2+}. A similar experiment was performed with both bacterial strains grown on TCTP control surfaces; increasing the concentration of free calcium had little effect on the proliferation, See Supplementary Material. These results suggest that as cells come into contact with the gel surface, essential metal ions are displaced from the cell wall surface and this may be the first step in the lytic mechanism that ultimately leads to cell death.

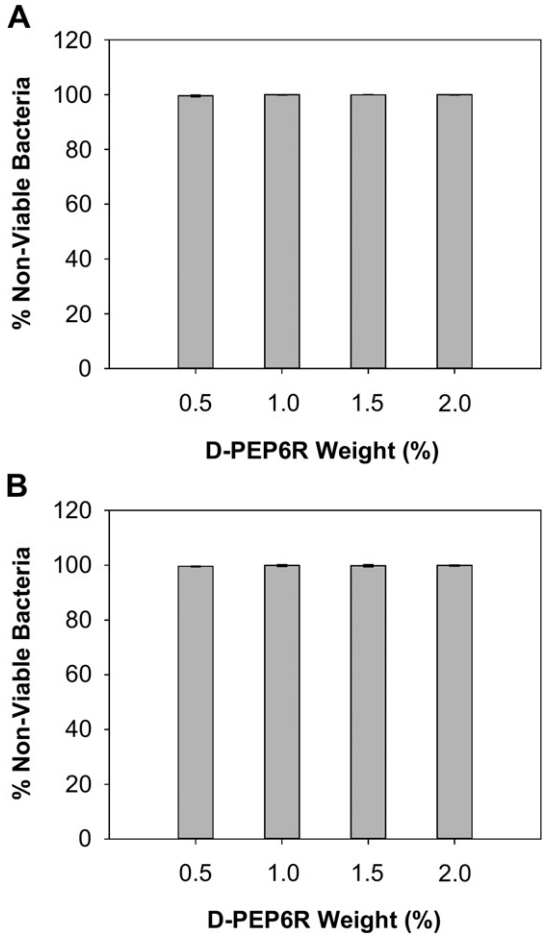

Fig. 8. Antibacterial activity of D-PEP6R hydrogel surfaces against *E. coli* (A) and *S. aureus* (B) after 24 h incubation at 37 °C. Percent non-viable bacteria is reported for 0.5, 1, 1.5, and 2 wt% hydrogels ($n = 3$).

Although all of the data support an antibacterial mechanism involving the surface of the hydrogel, the possibility that free soluble peptide may also contribute exists. In fact, close inspection of Fig. 7 shows that cells suspended above the gel's surface are also dead. These could be dead cells floating away from the surface after having been killed or these could be cells that have undergone cell death before engaging the surface. When the gels are initially formed from the self-assembling peptides, a small population of peptides do not get incorporated into the growing fibril network and remain freely diffusing in solution. We have found that the amount of soluble peptide that remains after gel formation is dependent both on the exact sequence of the peptide and the weight percent of its respective gel. Higher weight percent gels contain more soluble peptide. To investigate the possibility that freely diffusing peptide also contributes to the activity of the gels, the supernatant above freshly formed gels were tested for their ability to kill bacteria. The results demonstrate that the supernatant obtained from a 2 wt % gel is capable of killing 10^4 CFU/mL of *E. coli*. However, the supernatant obtained from 0.5 wt % are significantly less effective, which is consistent with less soluble peptide being available from this lower weight percent gel, See Supplementary Material. Given the fact that most of the arginine-rich gels examined in this study are extremely effective at 0.5 wt % and the supernatant derived from these gels are not, this strongly suggests that the lion's share of the activity is due to the gel's surface and, if available, soluble peptide can aid the fight.

3.5. PEP6R hydrogel displays optimal biological and material properties

The PEP6R gel displays potent activity against *E. coli* and *S. aureus* and multi-drug resistant *P. aeruginosa*. Activity which is

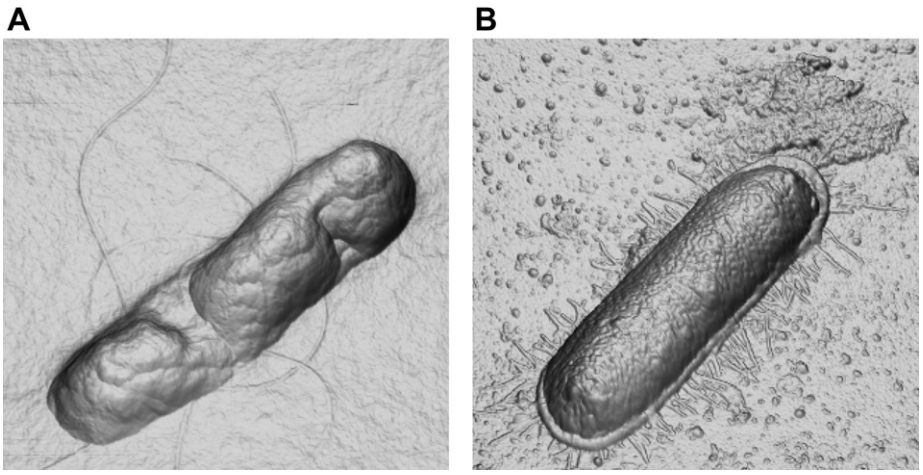

Fig. 9. Three-dimensional orthogonal projection images (derived from AFM height data) of *E. coli* cells on (A) 2 wt% PEP6R hydrogel surface and (B) poly-L-Lysine control surface after 2 h incubation at 37 °C.

balanced by low hemolytic potential. In addition to biological activity, the mechanical properties of a material are also important in defining its utility. Gels that can be introduced in vivo in a minimally invasive manner are especially useful. Gels prepared from PEP6R are shear-thinning, but have the ability to self-heal and thus can be delivered by simple syringe injection [34]. The shear-thin/recovery properties of the PEP6R gel are show in Fig. 12A. In this experiment, a dynamic time sweep is first

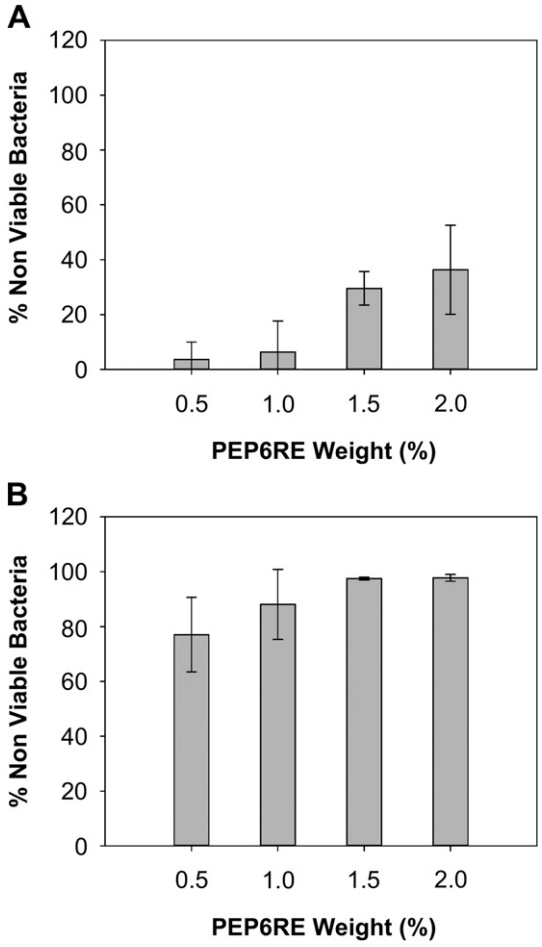

Fig. 10. Antibacterial activity of PEP6RE hydrogel surfaces against *E. coli* (A) and *S. aureus* (B) after 24 h incubation at 37 °C. Percent non-viable bacteria is reported for 0.5, 1, 1.5, and 2 wt% hydrogels ($n = 3$).

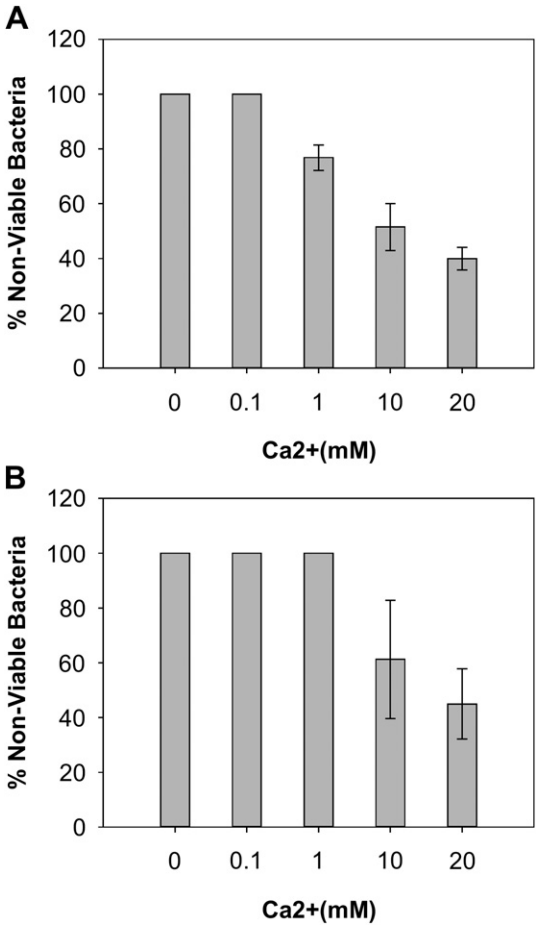

Fig. 11. Antibacterial activity of PEP6R hydrogel surfaces against *E. coli* (A) and *S. aureus* (B) in the presence of Ca^{2+}, after 24 h incubation at 37 °C. Percent non-viable bacteria is reported for 1 wt% hydrogels in the presence of 0, 0.1, 1, 10 and 20 mM of Ca^{2+} ($n = 3$).

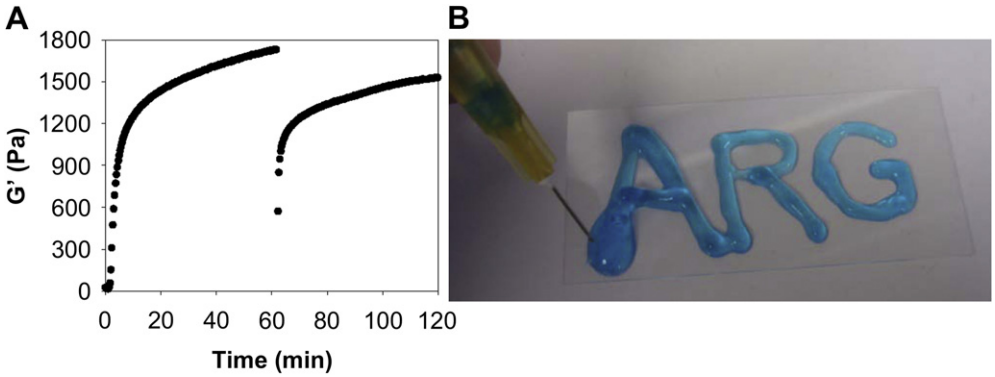

Fig. 12. (A) Shear-thin/recovery process monitored rheologically for a 1 wt% PEP6R hydrogel at 37 °C. Initial time sweep (6 rad/s and 0.2% strain) monitors gel formation for 1 h after gelation was initiated. Then, application of 1000% strain for 30 s, shear-thins the gel. Finally, a time sweep (6 rad/s, 0.2% strain) monitors hydrogel recovery for 1 h. (B) Photograph of a 1 wt% PEP6R hydrogel prepared in a syringe and shear-thin delivered to a vertical glass surface.

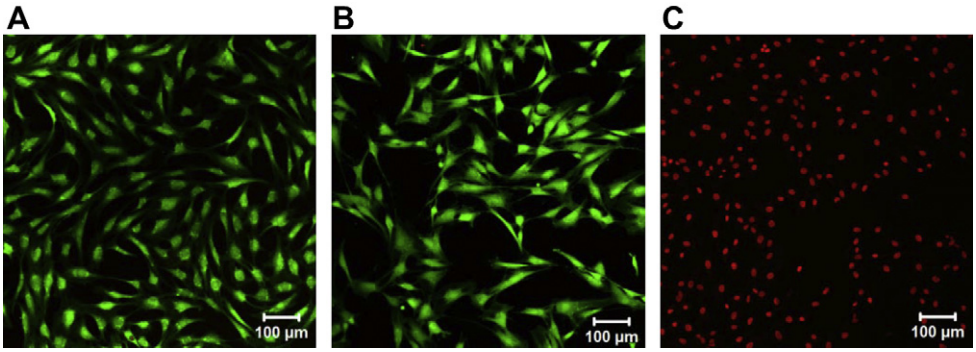

Fig. 13. Live-dead viability assay of mesenchymal C3H10t1/2 stem cells. LSCM images show the cells on: (A) the surface of 2 wt% PEP6R hydrogel, (B) a borosilicate control surface, and (C) a borosilicate control surface in the presence of 0.1% Triton X-100 solution (Scale bars: 100 μm; $n = 3$).

performed to monitor the initial formation of the gel on the rheometer at 37 °C. After 1 h, 1000% strain was applied to the gel for 30 s to thin the material. The immediate decrease in G′ indicates that the material has thinned and is capable of flow. After the cessation of high strain, another time sweep at low strain (0.2%, 6 rad/s) was performed to assess the material's ability to recover its mechanical integrity. The PEP6R gel is able to recover to about 90% of its initial mechanical rigidity after 1 h. The shear-thin and recovery rheological properties of the gel are macroscopically demonstrated in Fig. 12B. Here, the hydrogel if prepared directly within a syringe. Depressing the syringe plunger, thins the gel through the narrow-bore needle and on exiting the needle, the gel immediately recovers. Here the gel is delivered to a vertically-oriented glass surface where it stays resident at the point of application.

Lastly, the cytocompatibility of the PEP6R gel was assessed toward mammalian mesenchymal stem cells. Murine C3H10t1/2 mesenchymal stem cells have surfaces that contain a plethora of cell membrane proteins and sugars making these cells a good model of the membranes of most mammalian cells. Cells (20,000 cells/cm^2) were introduced to the surface of the PEP6R gel and incubated for 24 h at 37 °C and 5% CO_2. Fig. 13 shows a live-dead assay that clearly demonstrates that the cells are viable on the gel surface (A), as well as on a control borosilicate surface (B). The negative control in which cells are lysed with detergent is also shown (C). These results demonstrate that although the PEP6R gel is active against bacteria, it is selective and compatible toward the mammalian cells examined here.

4. Conclusions

A family of peptide-based hydrogels was prepared to investigate the importance of Arg content on their antibacterial, hemolytic and material rheological properties. The parent peptide, PEP8R is a 20-residue, amphiphilic β-hairpin peptide that self-assembles into a network of fibrils that define a moderately rigid hydrogel, which is potently active against *E. coli* and *S. aureus*. The peptide contains eight Arg residues whose side chains are displayed from its hydrophilic face, and in the self-assembled state, are displayed in high copy number from the solvent exposed surfaces of each fibril in the network. Although the PEP8R gel has excellent antibacterial properties, it is non-selective, showing lytic activity toward hRBCs. Three additional peptides, PEP6R, PEP4R, and PEP2R, were designed where pairs of Arg residues in PEP8R were sequentially replaced with Lys. Rheological studies show that decreasing the number of Arg residues to six, results in an increase in G′, but further reduction in Arg content results in a decrease in the gel's rigidity. Cell-based assays show that decreasing the Arg content results in a pronounced decrease in hemolytic activity and only a slight decrease in antibacterial activity. The optimal gel is composed of the PEP6R peptide, which contains six Arg residues. This syringe-deliverable gel is minimally hemolytic, cytocompatible toward mesenchymal stem cells, yet displays potent activity against gram-positive and gram-negative bacteria, including *P. aeruginosa*, a multi-drug resistant bacterium. Mechanistic studies suggest a mode of action that involves membrane disruption initiated by the dissociation of essential divalent metal ions from the bacterium's cell wall as it come into contact with the material's surface.

Acknowledgments

This work was supported by a Marie Curie International Outgoing Fellowship within the 7th European Community Framework Programme awarded to Ana Salome Veiga (PIOF-GA-2009-235154). ASV also acknowledges Fundação para a Ciência e a Tecnologia (Ministério da Educação e Ciência, Portugal) for Fellowship SFRH/BPD/43931/2008. This work is partially supported by a graduate fellowship awarded to Chomdao Sinthuvanich through the *Strategic Scholarship for Frontier Research Network* (SFR) from the Office of the Higher Education Commission, Ministry of Education, Thailand. Diana Gaspar acknowledges Fundação para a Ciência e a Tecnologia (Ministério da Educação e Ciência, Portugal) for Fellowship SFRH/BPD/73500/2010. This work was also supported by the Intramural Research Program of the National Cancer Institute of the National Institutes of Health. We thank Fundação para a Ciência e Tecnologia (FCT-MCTES, Portugal) for funding – PTDC/SAU-BEB/099142/2008. We acknowledge Dr. M.C. Branco for helpful discussions.

Appendix A. Supplementary material

Supplementary material related to this article can be found at http://dx.doi.org/10.1016/j.biomaterials.2012.08.046.

References

[1] Edwards R, Harding KG. Bacteria and wound healing. Curr Opin Infect Dis 2004;17(2):91–6.
[2] Siddiqui AR, Bernstein JM. Chronic wound infection: facts and controversies. Clin Dermatol 2010;28(5):519–26.
[3] Doyle JS, Buising KL, Thursky KA, Worth LJ, Richards MJ. Epidemiology of infections acquired in intensive care units. Semin Respir Crit Care Med 2011; 32(2):115–38.
[4] Sydnor ERM, Perl TM. Hospital epidemiology and infection control in acute-care settings. Clin Microbiol Rev 2011;24(1):141–73.
[5] http://textbookofbacteriology.net/themicrobialworld/Pseudomonas.html; 2012.
[6] Driscoll JA, Brody SL, Kollef MH. The epidemiology, pathogenesis and treatment of pseudomonas aeruginosa infections. Drugs 2007;67(3):351–68.
[7] Rolston KV. New antimicrobial agents for the treatment of bacterial infections in cancer patients. Hematol Oncol 2009;27(3):107–14.
[8] Wu DC, Chan WW, Metelitsa AI, Fiorillo L, Lin AN. Pseudomonas skin infection: clinical features, epidemiology, and management. Am J Clin Dermatol 2011; 12(3):157–69.
[9] Jones DS, Lorimer CP, McCoy CP, Gorman SP. Characterization of the physicochemical, antimicrobial, and drug release properties of thermoresponsive hydrogel copolymers designed for medical device applications. J Biomed Mater Res B Appl Biomater 2008;85(2):417–26.
[10] Li P, Poon YF, Li W, Zhu HY, Yeap SH, Cao Y, et al. A polycationic antimicrobial and biocompatible hydrogel with microbe membrane suctioning ability. Nat Mater 2011;10(2):149–56.
[11] Petratos PB, Chen J, Felsen D, Poppas DP. Local pharmaceutical release from a new hydrogel implant. J Surg Res 2002;103(1):55–60.
[12] Flores CY, Diaz C, Rubert A, Benitez GA, Moreno MS, Fernandez Lorenzo de Mele MA, et al. Spontaneous adsorption of silver nanoparticles on Ti/TiO2 surfaces. Antibacterial effect on pseudomonas aeruginosa. J Colloid Interface Sci 2010;350(2):402–8.
[13] Gao G, Lange D, Hilpert K, Kindrachuk J, Zou Y, Cheng JT, et al. The biocompatibility and biofilm resistance of implant coatings based on hydrophilic polymer brushes conjugated with antimicrobial peptides. Biomaterials 2011; 32(16):3899–909.
[14] Kurt P, Wood L, Ohman DE, Wynne KJ. Highly effective contact antimicrobial surfaces via polymer surface modifiers. Langmuir 2007;23(9):4719–23.
[15] Murata H, Koepsel RR, Matyjaszewski K, Russell AJ. Permanent, non-leaching antibacterial surfaces-2: how high density cationic surfaces kill bacterial cells. Biomaterials 2007;28(32):4870–9.
[16] Thome J, Hollander A, Jaeger W, Trick I, Oehr C. Ultrathin antibacterial polyammonium coatings on polymer surfaces. Surf Coat Technol 2003;174: 584–7.
[17] Salick DA, Kretsinger JK, Pochan DJ, Schneider JP. Inherent antibacterial activity of a peptide-based beta-hairpin hydrogel. J Am Chem Soc 2007; 129(47):14793–9.
[18] Salick DA, Pochan DJ, Schneider JP. Design of an injectable beta-hairpin peptide hydrogel that kills methicillin-resistant staphylococcus aureus. Adv Mater 2009;21(41):4120–3.
[19] Chan DI, Prenner EJ, Vogel HJ. Tryptophan- and arginine-rich antimicrobial peptides: structures and mechanisms of action. Biochim Biophys Acta 2006; 1758(9):1184–202.
[20] de Leeuw E, Rajabi M, Zou G, Pazgier M, Lu W. Selective arginines are important for the antibacterial activity and host cell interaction of human alpha-defensin 5. FEBS Lett 2009;583(15):2507–12.
[21] Schmidt NW, Mishra A, Lai GH, Davis M, Sanders LK, Tran D, et al. Criterion for amino acid composition of defensins and antimicrobial peptides based on geometry of membrane destabilization. J Am Chem Soc 2011;133(17): 6720–7.
[22] Tanabe H, Qu X, Weeks CS, Cummings JE, Kolusheva S, Walsh KB, et al. Structure-activity determinants in paneth cell alpha-defensins: loss-of-function in mouse cryptdin-4 by charge-reversal at arginine residue positions. J Biol Chem 2004;279(12):11976–83.
[23] Zou G, de Leeuw E, Li C, Pazgier M, Zeng P, Lu WY, et al. Toward understanding the cationicity of defensins. Arg and lys versus their noncoded analogs. J Biol Chem 2007;282(27):19653–65.
[24] Stanger HE, Syud FA, Espinosa JF, Giriat I, Muir T, Gellman SH. Length-dependent stability and strand length limits in antiparallel beta-sheet secondary structure. Proc Natl Acad Sci USA 2001;98(21):12015–20.
[25] Ozbas B, Rajagopal K, Schneider JP, Pochan DJ. Semiflexible chain networks formed via self-assembly of beta-hairpin molecules. Phys Rev Lett 2004;93(26 Pt 1):268106.
[26] Schneider JP, Pochan DJ, Ozbas B, Rajagopal K, Pakstis L, Kretsinger J. Responsive hydrogels from the intramolecular folding and self-assembly of a designed peptide. J Am Chem Soc 2002;124(50):15030–7.
[27] Adamopoulos L, Montegna J, Hampikian G, Argyropoulos DS, Heitmann J, Lucia LA. A simple method to tune the gross antibacterial activity of cellulosic biomaterials. Carbohydr Polym 2007;69(4):805–10.
[28] Lichter JA, Rubner MF. Polyelectrolyte multilayers with intrinsic antimicrobial functionality: the importance of mobile polycations. Langmuir 2009;25(13): 7686–94.
[29] Clejan S, Krulwich TA, Mondrus KR, Seto-Young D. Membrane lipid composition of obligately and facultatively alkalophilic strains of Bacillus spp. J Bacteriol 1986;168(1):334–40.
[30] Epand RM, Epand RF. Bacterial membrane lipids in the action of antimicrobial agents. J Pept Sci 2011;17(5):298–305.
[31] Kol MA, van Laak AN, Rijkers DT, Killian JA, de Kroon AI, de Kruijff B. Phospholipid flop induced by transmembrane peptides in model membranes is modulated by lipid composition. Biochemistry 2003;42(1):231–7.
[32] Madkour AE, Dabkowski JM, Nusslein K, Tew GN. Fast disinfecting antimicrobial surfaces. Langmuir 2009;25(2):1060–7.
[33] Gilbert P, Moore LE. Cationic antiseptics: diversity of action under a common epithet. J Appl Microbiol 2005;99(4):703–15.
[34] Yan C, Altunbas A, Yucel T, Nagarkar RP, Schneider JP, Pochan DJ. Injectable solid hydrogel: mechanism of shear-thinning and immediate recovery of injectable beta-hairpin peptide hydrogels. Soft Matter 2010;6(20):5143–56.